Taylor & Francis
Taylor & Francis Group

Journal of Toxicology and Environmental Health, Part A
Current Issues

ISSN: (Print) (Online) Journal homepage: www.tandfonline.com/journals/uteh20

Exposure to emissions generated by 3-dimensional printing with polycarbonate: effects on peripheral vascular function, cardiac vascular morphology and expression of markers of oxidative stress in male rat cardiac tissue

Kristine Krajnak, Mariana Farcas, Diana Richardson, Mary Anne Hammer, Stacey Waugh, Walter McKinney, Alycia Knepp, Mark Jackson, Dru Burns, Ryan LeBouf, Joanna Matheson, Treye Thomas & Yong Qian

To cite this article: Kristine Krajnak, Mariana Farcas, Diana Richardson, Mary Anne Hammer, Stacey Waugh, Walter McKinney, Alycia Knepp, Mark Jackson, Dru Burns, Ryan LeBouf, Joanna Matheson, Treye Thomas & Yong Qian (2024) Exposure to emissions generated by 3-dimensional printing with polycarbonate: effects on peripheral vascular function, cardiac vascular morphology and expression of markers of oxidative stress in male rat cardiac tissue, Journal of Toxicology and Environmental Health, Part A, 87:13, 541-559, DOI: 10.1080/15287394.2024.2346938

To link to this article: https://doi.org/10.1080/15287394.2024.2346938

JOURNAL OF TOXICOLOGY AND ENVIRONMENTAL HEALTH, PART A
2024, VOL. 87, NO. 13, 541–559
https://doi.org/10.1080/15287394.2024.2346938

Taylor & Francis
Taylor & Francis Group

Exposure to emissions generated by 3-dimensional printing with polycarbonate: effects on peripheral vascular function, cardiac vascular morphology and expression of markers of oxidative stress in male rat cardiac tissue

Kristine Krajnak[a], Mariana Farcas[a], Diana Richardson[a], Mary Anne Hammer[a], Stacey Waugh[a], Walter McKinney[a], Alycia Knepp[a], Mark Jackson[a], Dru Burns[b], Ryan LeBouf[b], Joanna Matheson[c], Treye Thomas[c], and Yong Qian[a]

[a]Health Effects Laboratory Division, National Institute for Occupational Safety and Health, Morgantown, WV, USA; [b]Respiratory Health Division, Morgantown, WV, USA; [c]Consumer Product Safety Commission, Rockville, MD, USA

ABSTRACT

Three-dimensional (3D) printing with polycarbonate (PC) plastic occurs in manufacturing settings, homes, and schools. Emissions generated during printing with PC stock and bisphenol-A (BPA), an endocrine disrupter in PC, may induce adverse health effects. Inhalation of 3D printer emissions, and changes in endocrine function may lead to cardiovascular dysfunction. The goal of this study was to determine whether there were any changes in markers of peripheral or cardiovascular dysfunction in animals exposed to PC-emissions. Male Sprague Dawley rats were exposed to PC-emissions generated by 3D printing for 1, 4, 8, 15 or 30 d. Exposure induced a reduction in the expression of the antioxidant catalase (*Cat*) and endothelial nitric oxide synthase (*eNos*). Endothelin and hypoxia-induced factor 1α transcripts increased after 30 d. Alterations in transcription were associated with elevations in immunostaining for estrogen and androgen receptors, nitrotyrosine, and vascular endothelial growth factor in cardiac arteries of PC-emission exposed animals. There was also a reduction eNOS immunostaining in cardiac arteries from rats exposed to PC-emissions. Histological analyses of heart sections revealed that exposure to PC-emissions resulted in vaso-constriction of cardiac arteries and thickening of the vascular smooth muscle wall, suggesting there was a prolonged vasoconstriction. These findings are consistent with studies showing that inhalation 3D-printer emissions affect cardiovascular function. Although BPA levels in animals were relatively low, exposure-induced changes in immunostaining for estrogen and androgen receptors in cardiac arteries suggest that changes in the action of steroid hormones may have contributed to the alterations in morphology and markers of cardiac function.

KEYWORDS

Inhalation; polycarbonate emissions; cardiovascular morphology; cardiovascular function; three-dimensional (3D) printing; particulate matter

Introduction

Three-dimensional (3D) printing is increasingly being used in large manufacturing settings, small manufacturing settings located in homes that make products to be sold, and schools (Abraham and Chakraborty 2019; Shivika and Subhankar 2017; Stefaniak, du Preez, and du Plessis 2021). A diverse range of items may be produced using 3D printers, including machinery parts, novelty items, pharmaceuticals, and even houses (Yi et al. 2016). Fused deposition modeling (FDM) 3D printers are the most widely used systems with standard thermoplastics such as acrylonitrile butadiene styrene (ABS), polylactic acid and polycarbonate (PC) commonly used in the manufacturing processes (Farcas et al. 2019, 2020). Heating of the thermoplastics generate and release particulate and fumes. Emission constituents frequently measured include particle number, aldehydes, benzene, toluene, ethylbenzene, and xylenes (Väisänen et al. 2022; Stefaniak et al. 2017). Inhalation of the emitted particulate and/or the fumes may pose adverse health effects to users of these systems as well as bystanders (Johnson 2013; Rochester 2013; Shivika and Subhankar 2017; Stefaniak et al. 2017; Stephens et al. 2013; Tarskikh, Klimatskaya, and Kolesnikov 2013).

Exposure to emissions generated during printing with ABS results in decreased responsiveness of the vascular system to vasodilating factors (Hubbs et al. 2011; Stefaniak et al. 2017). Because the disposition of plastic nano-particulate *in vivo* is not known, it is difficult to determine whether the vascular responses observed were due to inhalation of particulate, or to volatile organic compounds

CONTACT Kristine Krajnak ksk1@cdc.gov Health Effects Laboratory Division, National Institute of Occupational Safety and Health, 1000 Fredrick Lane, Morgantown, WV 26508, USA

(VOCs) released during the heating and printing process. Several investigators demonstrated that inhalation of ABS (Hubbs et al. 2011; Stefaniak et al. 2017; Yi et al. 2016) and ingestion or dermal absorption of PC-plastic (Lehmler et al. 2018, Kim et al. 2020; Rochester 2013) affected both peripheral and cardiovascular systems by making them less sensitive to factors that induce vasodilation (Stefaniak et al. 2017). Because PC-plastic is routinely used for 3D-printing in assorted settings including workplaces, homes, schools or libraries, it is important to determine whether inhalation of PC-emissions affects cardiovascular function.

Polycarbonate emissions might also include bisphenol A (BPA). Bisphenols are known to be endocrine and metabolic disruptors as these substances interfere with actions of steroid and thyroid hormones and are reported to exert significant effects on a number of physiological systems including the endocrine and cardiovascular systems (Lehmler et al. 2018; Ma et al. 2019; Kim et al. 2020). Because steroid hormones exert major effects on cardiovascular functions, it is possible that inhalation of PC particulate and/or BPA might impact cardiovascular functions. Estrogen in females, and testosterone in males, may exert protective effects on both heart function and on peripheral vascular health by regulating heart rate, blood pressure, and vascular responses to various stressors (Huxley 2007; Lundberg et al. 1990). *In vitro* binding studies demonstrated that BPA displays a 10-fold higher affinity for estrogen receptors than estradiol, and therefore exposure to bisphenols may alter the protective effects of estrogen on the cardiovascular system (Huxley 2007; Lundberg et al. 1990). Similarly, beneficial effects of testosterone on the cardiovascular system may be inhibited since bisphenols also might affect the activity of testosterone on heart and peripheral vascular system by binding to androgen receptors (Huxley 2007; Khraishah et al. 2022; Lundberg et al. 1990). Inhalation of PC plastic emissions or BPA might also alter development of the cardiovascular system in children that are exposed at school or at home if the home is serving as a small manufacturing environment by acting on endocrine systems that play a role in cardiovascular development in children and by generally affecting heart development (Lehmler et al. 2018; NTP 2021; Stephens et al. 2013). In addition, low doses of bisphenols reduce 5α-reductase levels, resulting in effects on steroid hormone synthesis and increased aromatase levels leading to an elevated risk of prostate cancer occurrence (Sanchez et al. 2022). At present it is not known if changes in steroid hormone levels induced by PC-emissions and/or inhalation of BPA might act to affect cardiovascular function.

Local and systemic inflammation and increases in oxidative activity may result from inhalation of particulate matter (PM) (Hubbs et al. 2011; Stefaniak et al. 2017; Tarskikh, Klimatskaya, and Kolesnikov 2013; Yi et al. 2016). Systemic changes may result in inflammatory factors, such as interleukin 1β (Il1β) and α tumor necrosis factor α (TNF-α), and inflammatory cells, such as macrophages and monocytes, being transported through the circulatory system to act at other sites in the body, including the cardiovascular system, and alter function at these sites (Hubbs et al. 2011). These inflammatory cells may generate cytokines and reactive oxygen species (ROS) that affect various tissues, or might stimulate tissues to produce these factors. Recently (Farcas et al. 2024), examined the influence of inhaling PC-emissions and found that inhalation of these emission did not result in marked pulmonary or systemic inflammation. Based upon these findings, it is likely that the effects of inhaling PC-emissions might involve other mechanisms. Inhaled PM might also be translocated from the lung and enter the circulatory system, where it may induce inflammation or act on other physiological systems in the body (Hubbs et al. 2011). However, because the fate of nanoscale plastics in the body in comparison to larger size particles is not well studied, and size of PM inhaled may initiate a significant effect on their disposition once in the body, examining the effects of inhaling emissions on other systems is important because these other physiological systems may be affected, independently of the influence on the respiratory system. Finally, PM-bound chemicals may be released in bodily fluids, and subsequently induce alterations in physiological functions.

To determine if inhalation of PC-emissions generated during 3D printing affects the cardiovascular system, the current study examined the effects of inhaling PC-emissions after 1-, 4-, 8-, 15-, or 30-

d exposure, on peripheral vascular responses to vaso-modulating agents, on cardiac morphology and on expression of proteins and transcripts that are markers of inflammation, oxidative stress and cardiovascular dysfunction. More specifically, based upon previous data, it was postulated that inhalation of PC-emissions might result in an elevation in markers of oxidative stress and induction of vasoconstriction, which in the long-term may serve as a risk factor for development of high blood pressure and cardiovascular diseases.

Methods

Animals

Male Sprague Dawley rats ([H1a: (SD) CVF, $n = 6$ rats/group; 6–7 weeks of age, 200–250 g) were obtained from Hilltop Lab Animals, Inc., Scottdale, PA. Animals in this study were part of a larger study examining the effects of PC-emission inhalation on a number of different physiological systems. Because this was the first study, characterizing the effects of PC-emission inhalation on a number of different physiological systems, only males were included. All animals were free of viral pathogens, parasites, *mycoplasms*, *Helicobacter*, and cilia-associated respiratory (CAR) bacillus. Rats were acclimated to the facilities for 1 week after arrival. All animals were housed in cages ventilated with HEPA-filters under-controlled temperature and humidity conditions and a 12 h light/dark cycle. Food (Teklad 7913) and tap water were provided *ad libitum*. The animal facilities are pathogen-free, environmentally controlled, and accredited by AAALAC International. All procedures were approved by the CDC Morgantown, WV Animal Care and Use Committee and are in compliance with the Public Health Service Policy on Humane Care and Use of Laboratory Animals and the NIH Guide for the Care and Use of Laboratory Animals.

Exposure

After 1 week of acclimation to the facility, animals were exposed to filtered-air (controls) or PC-emissions generated by 3D printing as described in (Farcas et al. 2019, 2024; Krajnak et al. 2023). Animals were placed in separate compartments of a whole-body exposure chamber that held up to 12 animals. No food or water was available during the exposure. The cage rack with the animals rested on top of cage support beams which had 1 cm outside diameter stainless steel tubes with small holes. Each hole was placed in the center of the cage partition so that aerosols would be drawn into the breathing space. Three desktop 3D printers (LulzBot Mini, Fargo Additive Manufacturing Equipment 3D LLC, Fargo, ND) were placed in an airtight chamber. Black polycarbonate filament (Gizmo Dorks LLC, Temple City, CA 3D Printing Polycarbonate Filament – Gizmo Dorks) was fed into each printer, which operated continuously during the 4 h exposure period. At the beginning of each exposure, animals were placed into the designated chamber (for air or PC emission exposure). Emissions from the printing chamber or filtered air were pumped into the whole-body inhalation chamber. At the end of each exposure, animals were placed into their home cages and returned to the colony room.

Emissions generated by the printers were discharged into the chamber with the animals. While printing, the print nozzle temperature was 290°C and the bed temperature was 120°C (Farcas et al. 2024; Krajnak et al. 2023). The mean hydrodynamic particle size and particle concentrations were measured using nanoparticle tracking system analysis (NTA; NanoSight NS300, Malvern Instruments, Worcestershire, UK). The measured particulate emissions inside the exposure chamber averaged approximately 0.592 mg/m^3 (or approximately 600,000 particles/cm^3) of particulate for a 4 h exposure when the mean was calculated over all days of treatment. The actual average mass concentration determined with gravimetric filters over all exposure days was 592 µg/m^3 with a daily average standard deviation of 200 µg/m^3. Particulate was also collected every 5 sec and particle size was measured using a fast mobility particle sizer (size range 5.6–560 nm, model 3091 TSI Inc, Shoreview MN). The particle size distribution was converted to aerodynamic equivalent mass by assuming all particles were spherical and displayed a density of 1.2 g/cm^3 (the density of polycarbonate). The mean aerodynamic equivalent diameter measured inside the exposure chamber during the print jobs was 40 nm. The PC particles

were also collected on filters and imaged with a scanning electron microscope. Typical physical diameters for PC particulate ranged from 40 nm up to 90 nm (Farcas et al. 2019). Particle concentration and particle size are similar to those reported in a University Makerspace study (450,000 particles/cm^3; Secondo et al. 2020).

Variations of particle emissions over the 4 h print job might be affected by several factors: 1) build plates were heated and this could cause the extruded plastic to cool faster the farther away it is from the 1st print layer; 2) 3-D printing housing chamber is not temperature controlled thus the air temperature inside this chamber would rise during print jobs, and 3) variations of filament composition during the manufacturing process could also play a role. The precise chemical composition of each roll of filament is proprietary. Generating the exact same mass concentration in the exposure chamber each day proved to be difficult, partly because 3 printers were being used and the odds of having one of them experience failed print before completion was significant. Prints failed if the part did not stay attached to the build plate, the print nozzle became clogged, or there was a software error with the printer. If a printer failed during an exposure, that printer would be stopped to prevent damage to the printer. A printer could not be restarted because that would require the printer housing chamber door to be opened. This would dilute the concentration of the emissions down to near zero mid exposure while trying to fix the printer.

Analysis of volatile organic compounds by GC/MS

The volatile organic components of the PC emissions were analyzed by GC/MS from samples collected over a 4 h collection period (Table 1). The measurement of volatile compounds was conducted using a method published in the NIOSH Analytical Methods Manual (2018; 3900: Volatile organic compounds (VOC), C1 to C10 canister method; are found at https://www.cdc.gov/niosh/nmam/default.html). The levels of measured compounds were low, with acetaldehyde, acetone, ethanol, and ethylbenzene levels being the highest among the detected compounds. Table 1 presents the levels (ppb) of VOC measured in this study and Occupational Safety and Health Administrations (OSHAs) permissible exposure limits (PELs). None of the compounds measured in this experiment were above the OSHA PELs.

BPA and bisphenol A diglycidyl ether were also assessed in the PC-emissions. Samples were collected as described in (Krajnak et al. 2023). Particulate matter was collected over a 4 h period at 1 L per/min onto glass fiber filters (SKC lot #21600-7E5-274; $n = 6$ samples) from chambers where the particulate concentration in the air was approximately 0.6 mg/m^3. The filters were then analyzed by BVNA labs (Novi, MI). The average concentration of bisphenol in the samples was 5.3 ± 0.18 µg. Using a mass particle distribution model to determine BPA deposition in nose, trachea, alveolae and lung (where the tidal volume is 1.7 ml, the breathing rate is 120 breaths/min and the exposure time is 240 min), the estimated daily deposition of BPA in the entire respiratory tract was 36 ng. Bisphenol A diglycidyl ether was not detectable in any of the samples.

Tissue collection

Groups of animals (6 air control and 6 treated) were euthanized by injection of pentobarbital (100–300 mg/kg i.p.) followed by exsanguination 24 hr after 1, 4, 8, 15 or 30 d treatment. Heart tissue was collected, fixed in 10% formalin, and processed for histological and immunohistochemical analyses

TABLE 1. This Table Shows Concentrations of Various Volatile Chemicals in 4 H of Emissions. Measurements Are Average Parts per Billion (Ppb) During a Single 4 h Exposure, the Standard Deviation of the 4 Measurements and the OSHA Permissiblelimits for Each Compound in Ppb

Compound	Mean (ppb)	std	OSHA PEL (ppb)
2,3-Butanedione	<0.3	0	na
2,3-Hexanedione	<0.4	0.00	na
Acetone	1573.8	1431.47	1,000,000
Acetonitrile	1.0	0.35	40,000
Benzene	1.0	0.15	1,000
Chloroform	<0.1	0.00	50,000
D-Limonene	2.5	0.42	na
Ethanol	22.4	2.39	1,000,000
Ethylbenzene	<0.3	0.00	100,000
Isopropyl Alcohol	13.6	4.12	400,000
Methyl Methacrylate	2.0	1.22	100,000
Methylene Chloride	<0.2	0.00	25,000
Styrene	2.7	0.44	100,000
Toluene	<0.3	0.00	200,000
alpha-Pinene	<0.5	0.00	na
m,p-Xylene	1.5	0.25	100,000
n-Hexane	<0.4	0.00	500,000
o-Xylene	1.2	0.20	100,000

to search for morphological changes, alterations in various protein concentrations, or for qRT-PCR to measure changes in transcript expression. Ventral tail arteries were also dissected and vasoconstriction and vasodilation in response to phenylephrine and acetylcholine were immediately measured in a microvessel system (Scincta, Ontario).

Tissue preparation: histology and immunohistochemistry

The heart was dissected from each animal. Each sample was fixed in 10% formalin for 24 h, paraffin embedded and sections (5 µm) were cut on a microtome. Five slides were collected from each animal, with each slide containing 1–2 tissue sections. One set of sections was stained with Harris hematoxylin and eosin (H&E) for histological analyses (assessment of number of inflammatory cells in cardiac muscle, arterial internal and external diameter, and muscle thickness). The other sections were stored in boxes until used for immunohistochemical identification of steroid receptors, oxidative stress markers and vascular remodeling.

Slides used for immunohistochemistry were deparaffinized by heating slides at 60°C in an oven and then putting them through 2–20 min rinses with xylene, and a descending series of ethanol rinses to remove the paraffin. Sections were then placed and kept in water to rehydrate the sections prior to immunohistochemistry. Antibody retrieval was performed by placing slides into 0.5 M citrate buffer and microwaving for approximately 5 min (4 × 1 min 20 sec intervals at the lowest power to prevent the citrate buffer from boiling over). Slides were then incubated in fresh citrate buffer for an additional 5 min, rinsed briefly with water, and then with 0.1 M phosphate buffered saline (PBS: pH 7.4).

Immunohistochemistry

Immunohistochemistry was performed using a modification of the protocol described in (Hubbs et al. 2011; Krajnak et al. 2023; Stefaniak et al. 2017). Briefly, a liquid proof barrier was drawn around tissue sections on each slide to keep all solutions on the tissues. Two hundred µl of each solution was pipetted onto tissue sections within the liquid proof barrier. Endogenous peroxidase activity was reduced by incubating tissues in 0.3% hydrogen peroxide in methanol for 20 min then rinsing with 0.1 M PBS (3 × 5 min rinses). Sections were then incubated in primary antibody diluted in normal serum and PBS + 0.3% Triton-X 100 overnight in humidified chambers at 4°C. The primary antibodies used were all purchased from Santa Cruz Biotechnology (Dallas, TX) and included mouse-anti estrogen receptor (ER), nitrotyrosine, inducible nitric oxide synthase, (iNOS), endothelial NOS (eNOS), androgen receptor (AR) and vascular endothelial growth factor (VEGF). Sections were then rinsed 3 × in PBS and incubated in the appropriate, fluorescently labeled secondary antibody (Jackson Immunolabs, Fisher Scientific, Pittsburgh, PA) for 1 h at room temperature. All slides were then rinsed in 0.1 M PBS, and the process was repeated with another primary antibody. After completion of the secondary antibody step, sections were air dried in the dark, cover slipped with Fluorogold containing 4′,6-diamidino-2-phenylindole (DAPI) mounting media (Fisher Scientific, Pittsburgh, PA) and stored at 4°C.

Microscopy

For immunostaining, multiple photomicrographs of arteries were taken at 20× magnification. ImageJ was used to quantify the immuno-stained area using previously published methods (Krajnak, Waugh, et al. 2006, 2010, 2013). All photos for a specific antibody were taken at the same intensity such that the area labeled and intensity of the labeling might be measured using Image J (NIH, Bethesda, MD). To measure labeled area and intensity of labeling in the endothelial cells and vascular smooth muscle (VSM), the inside of the lumen was circled and a measurement of the labeled area was made using Image J. This was followed by drawing another circle along the internal elastic membrane, and labeled area measured. The area of the lumen was subtracted from the area containing the elastic membrane, and this number was used as an estimate of endothelial cell labeling (Figure 1). Similar steps were performed to estimate VSM labeling; measures collected after outlining the elastic membrane and lumen of the artery were subtracted from measures made after outlining the whole artery and this number was utilized as the staining of the VSM. An average of the measures from each photo was calculated and this mean used for analyses (Krajnak et al. 2010).

H&E staining was also performed on one set of sections. Arteries were located within the tissue and photomicrographs of arteries were taken at 20 × magnification. The internal and external perimeters of 5 randomly selected arteries in the lateral atria and ventricles were selected for analyses. The ratio of the internal to external diameter was calculated. In addition, 4 measures of arterial wall muscle thickness were collected from each artery and averaged. The number of inflammatory cells and number of vacuoles in endothelial cells was also counted in each photomicrograph. The number of vacuoles within endothelial cells was employed as a measure of injury as evidenced by a rise in vacuoles equivalent to endothelial cell injury (Curry et al. 2005). The average number of each quantified structure per section was calculated and used for analyses.

Microvessel physiology

Tails were dissected from rats after exsanguination and placed in cold Dulbecco's modified Eagle's medium with glucose (Invitrogen/Gibco; Carlsbad, CA). Ventral tail arteries from the C18–20 region of the tail were dissected, mounted on glass pipettes in a microvessel chamber (Living System; Burlington, VT), and perfused with bicarbonated HEPES buffer (130 mM NaCl, 4 mM KCl, 1.2 mM $MgSO_4$, 1.8 mM $CaCl_2$, 10 mM HEPES, 1.80 mM KH_2PO_4, 0.03 mM EDTA, plus 10% glucose) warmed to 37°C. Arteries were pressurized to 60 mm Hg and allowed to equilibrate for approximately 1 hr. After the 1h acclimation period, the chamber buffer was replaced with fresh HEPES buffer and responsiveness of the arteries to phenylephrine (PE)-induced vasoconstriction and acetylcholine (ACh)-induced re-dilation was measured. All chemicals for microvessel exposures were purchased from Sigma (Indianapolis, IN) unless otherwise noted. To assess the effects of treatment on sensitivity to α_1-adrenoreceptor-mediated vasoconstriction, PE was added to the chamber such that changes in concentration occurred in half-log increments (−9 to −5.5 M) and the internal diameter of the artery was recorded after the arteries stabilized (approximately 5 min between concentrations). After measuring the dose-dependent vasoconstriction that occurred in response to PE, the chamber buffer, was removed and replaced with fresh, oxygenated HEPES buffer. After rinsing in oxygenated HEPES buffer for 15 min, arterial diameter returned to near baseline levels. Because ventral tail arteries usually display little basal tone, endothelial-mediated re-dilation was assessed after arteries were pre-constricted to approximately 50% of their baseline diameters with PE. In a pilot study, results demonstrated that re-constricting arteries with PE did not markedly affect subsequent responses to ACh or other vasomodulating factors. To assess the dilatory effects of ACh, the agonist was added cumulatively in half-log increments (−10 to −5 M) and changes in the internal diameter of the vessel measured as described for PE. The doses used are in the range of doses that induce vasoconstriction or dilation in ventral tail arteries as described in a number of studies (Krajnak, Dong, et al. 2006, 2020, 2022).

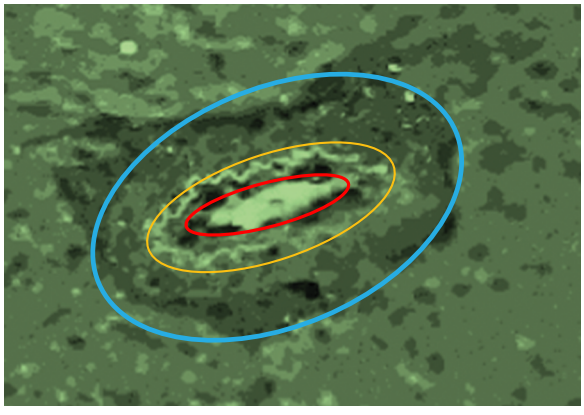

FIGURE 1. This photomicrograph depicts a cardiac artery. The circles are drawn to represent the different regions in which immune-labeling was quantified; red = internal perimeter, yellow endothelial perimeter and blue perimeter of the artery. The outlines in this figure are representative of the outlines that were made in image J. The outlines in ImageJ closely followed the contours of the tissue which were not perfect ovals.

Quantitative reverse transcriptase-polymerase chain reaction (qtRT-PCR)

qRT-PCR was performed to determine if exposure to PC-emissions resulted in alterations in transcript levels in heart tissue (Krajnak et al. 2013). Heart tissue was collected and fixed in 10% formalin for 24 h prior to being paraffin embedded and sectioned. RNA was extracted from eight 5 µm sections using the RNeasy FFPE Kit (Catalogue number 73,504: Qiagen, Valencia, CA). First strand

cDNA was synthesized from 1 mg total RNA using a Reverse Transcription System (Invitrogen, Carlsbad, CA). Because it was possible to only isolate a limited amount of RNA from paraffin-embedded sections, transcripts for factors that changed in response to inhalation of other types of particulate or toxic fumes were selected for analyses (Hubbs et al. 2011; Krajnak et al. 2017, 2023; Roberts et al. 2014). In the current study, qRT-PCR for the antioxidant enzyme *catalase (Cat)*, *endothelial nitric oxide synthase (eNOS), endothelin-1a (Et1a), hypoxia-induced factor-1(Hif1)* and *vascular endothelial growth factor (Vegf)* was performed. To determine if the treatment resulted in a change in transcript levels, fold changes from the same day controls were calculated. This was accomplished by calculating the average response for the control group and then subtracting the individual CT values for each sample from the mean of controls. A housekeeping gene (18_s) was used to determine if the changes in overall RNA concentrations in samples from different groups occurred.

Data analyses

PCR, histological and immunohistological data were analyzed using 2 (condition) x 3 (days of exposure; 1, 15 and 30) ANOVA. Post-hoc tests were conducted using t-tests or appropriate ANOVA. Planned comparisons were also run at each time point for specific factors because prior to the beginning of the experiment, it was predicted that there might be treatment-related differences in these factors with exposure to PC-emissions. Microvessel data were analyzed using 2 (condition) x 10 (dose) repeated measures ANOVAs. Jmp 15 (SAS, North Carolina). To identify the ED_{50} for PE and ACh, for each artery, % changes in internal diameter of the vessels at each dose were analyzed using a non-linear regression model for agonists in Graphpad (Prism 4). The ED_{50} were compared in control vs exposed animals using a Student's t-test. Differences with $p < 0.05$ were considered significant.

Results

Microvessel responses

Exposure to PC-emissions resulted in minimal effects on PE-induced vasoconstriction (Figure 2). After 1- and 8-d treatments (Figure 2a,e), there was a significant increase in sensitivity to PE-induced vasoconstriction, and the concentration of PE that initiated a 50% constriction (ED_{50}) was lower in the ventral tail artery of PC-emissions-exposed animals than controls (Figure 2b,f). This difference was not maintained on other days of the experiment. Exposure to PC-emissions did not markedly alter re-dilation in response to ACh (Figure 3).

Coronary morphology

One slide from each animal containing 1–2 sections of heart tissue was stained with H&E (Figure 4a-f). Mean (± sem) internal and external artery diameters for each day are presented in Table 2. Exposure to PC-emissions produced a reduction in the ratio of internal to external diameter of coronary arteries (Figure 4g). This ratio was significantly decreased in both control and exposed animals after 15d exposures as compared to 1 d; however, the reduction was only significant in control animals. After 1- and 30-d exposures a reduction in internal to external ratio in PC-emission exposed as compared to controls was observed.

The thickness of coronary smooth muscle arteries was also affected by exposure to PC-emissions (Figure 4h). One day following treatment a decrease in the thickness of coronary arterial smooth muscle in animals exposed to PC-emissions was detected. However, after 15-and 30-d exposure, smooth muscle thickness returned to control levels. The number of endothelial cells with vacuoles and inflammatory cells in artery tissue exhibited minor fluctuations. There were no marked alterations in parameter measures collected on cardiac muscle.

qRT-PCR

PCR was performed on sections collected from paraffin embedded heart tissue (Table 3). Exposure to PC-emissions resulted in a reduction in *eNOS* transcript gene expression levels after 15- and 30-d treatment, and decrease in *Cat* transcript gene expression levels after 30-d exposure as compared to tissue from air-exposed animals. Cardiac tissue from PC-emission exposed rats also showed elevation in *Et1a* and *Hif1* transcript gene expression levels after 30-d treatment as compared to air-exposed animals.

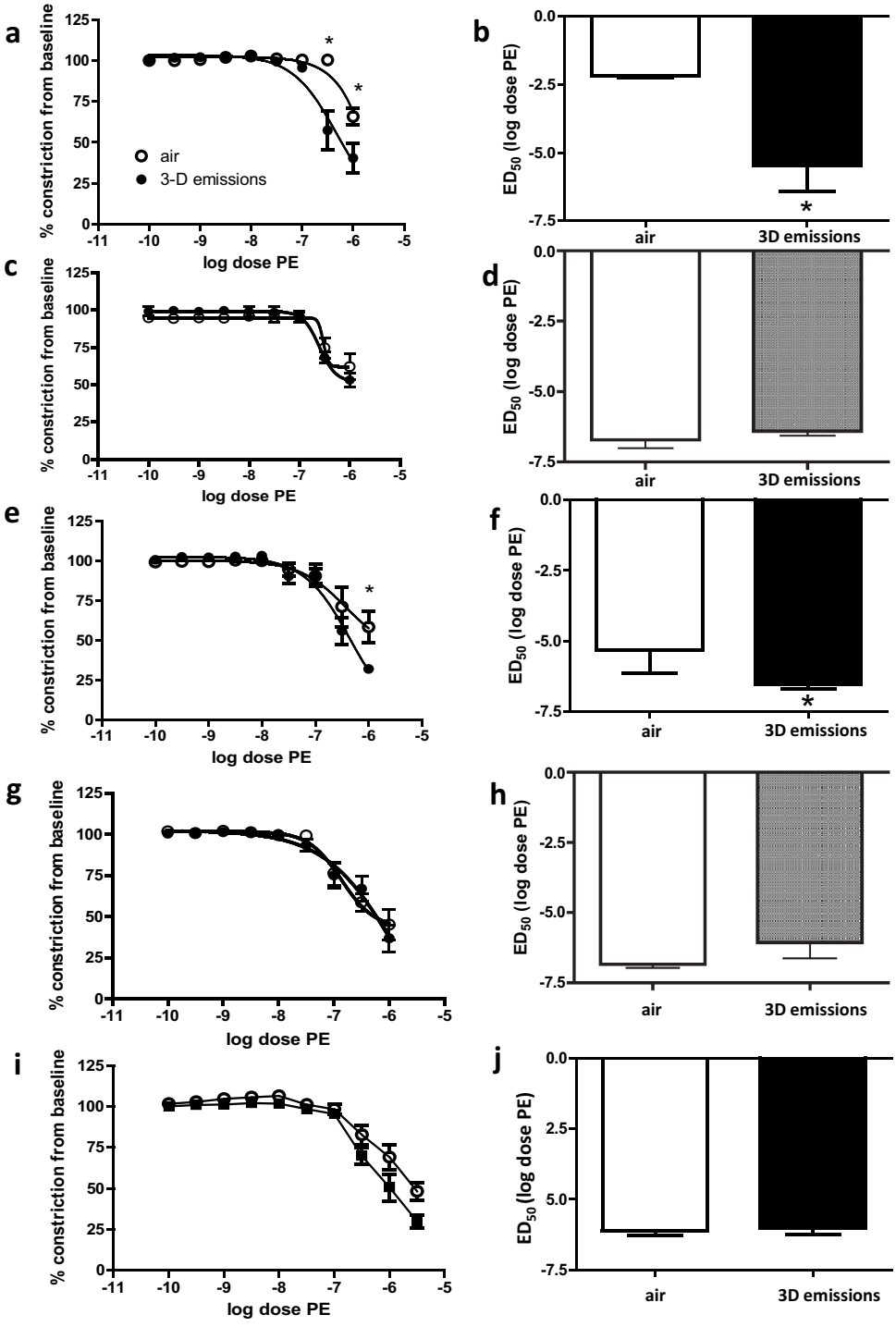

FIGURE 2. Changes in the internal diameter (mean ± SEM) of the ventral tail artery in response to phenylephrine (PE), after 1 (a, b), 4 (c, d), 8 (e, f), 15 (g, h) and 30 d (i, j) exposures to air or PC emissions. After 1- and 8-d exposures, arteries from PC animals were more sensitive to the vasoconstricting effects of PE at the highest dose, and the ED_{50} for PE-induced vasoconstriction occurred at a lower concentration in PC-exposed animals (*$p < 0.05$). There were no other marked changes in sensitivity to PE-induced constriction or the ED_{50} on any other day of the experiment.

Immunohistochemistry

A description of how immunohistochemical labeling in the endothelial layer and the VSM was quantified is presented in Figure 1. After 1-d exposure, there was no significant change Erα labeling in the endothelium of the heart (Figure 5a,b,m). However, the % area in the VSM of the heart immunolabeled for Erα was significantly higher in PC-emission

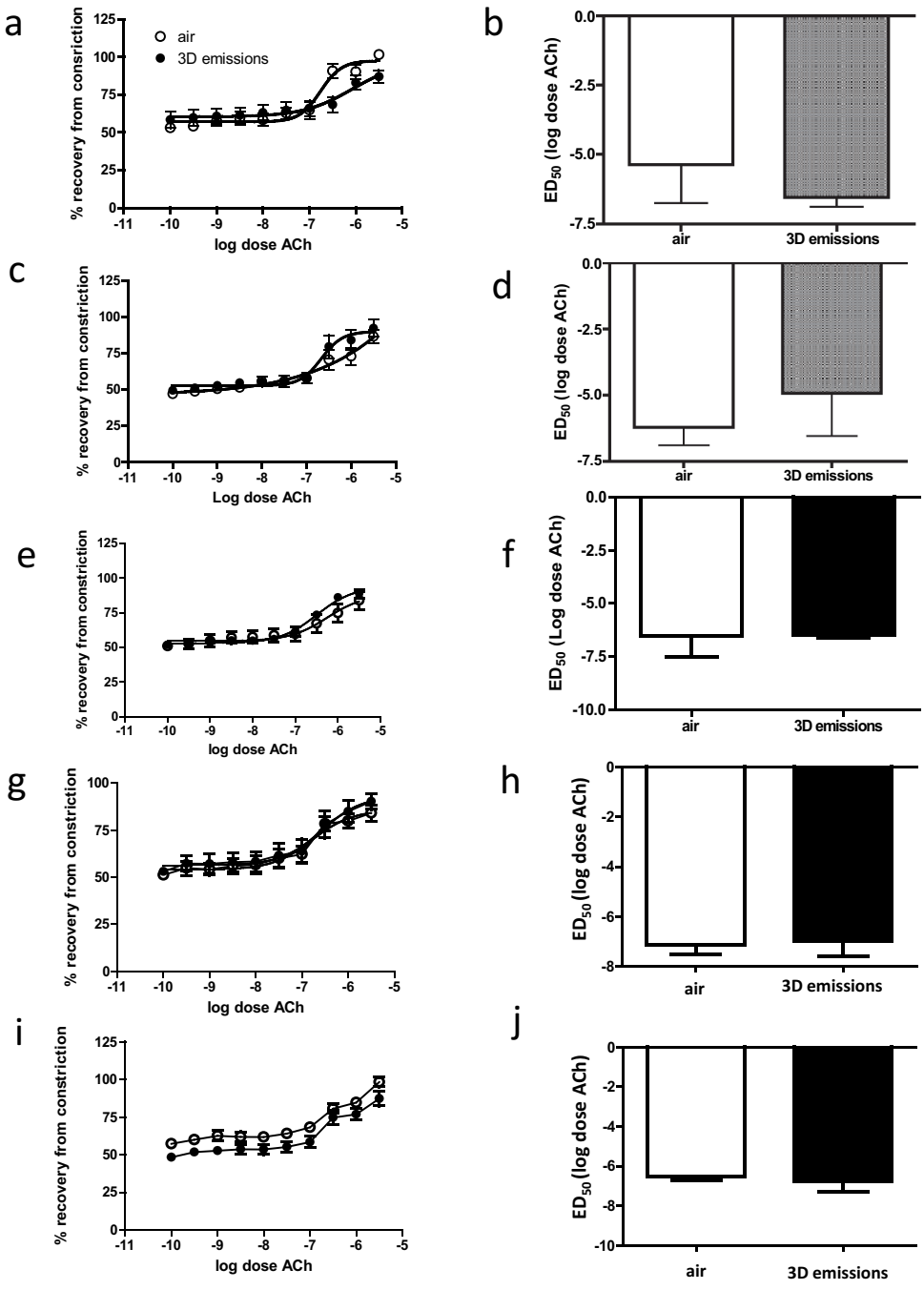

FIGURE 3. Changes in internal diameter (mean ± SEM) of the ventral tail artery in response to acetylcholine (ACh) after 1 (a, b), 4 (c, d), 8 (e, f), 15 (g, h) and 30 d (i, j) exposure to air or PC emissions. There were no significant alterations in ACh-induced re-dilation on any day of the experiment.

exposed than air-exposed animals after 1-d exposure (Figure 5a,b,n). However, after 15-d exposure to PC-emissions, Erα-receptor labeling was increased in the endothelium as compared to air controls and day 1 PC-emission exposed animals (Figure 5c,d,m). Thirty days following treatment, Erα-receptor labeling was enhanced in the endothelium of PC-emission exposed rats when compared 1 d air-exposed animals and same day air controls (Figure 5e,f,m). Erα was not markedly altered in the VSM of arteries after 15- and 30-d exposures to air and PC-emissions.

Nitrotyrosine labeling was also affected after exposure to PC-emissions (Figure 5g-l,o,p). In the

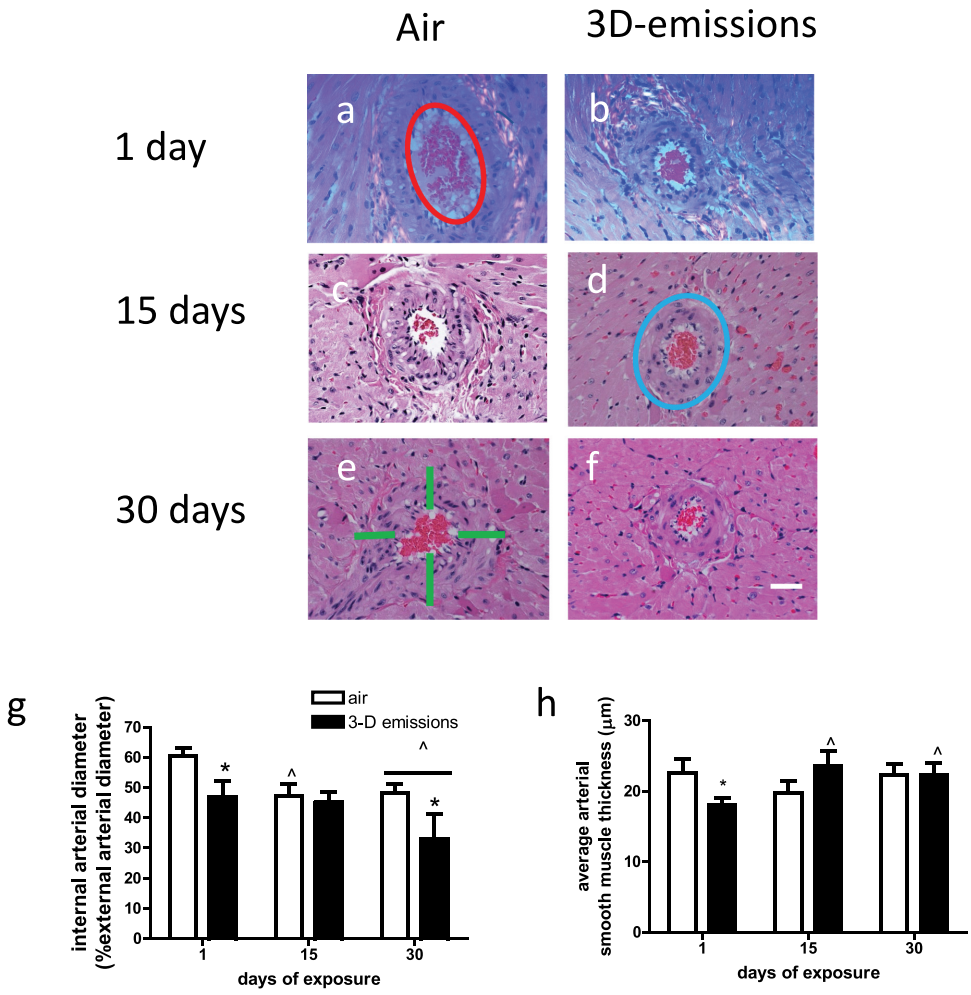

FIGURE 4. Photomicrographs of cardiac arteries (A-F) on days 1, 15 and 30 of exposure to air or PC emissions. The perimeter of the lumen (represented by the red circle in A) as a % of the external perimeter (the blue circle in D) of arteries decreased over time in both air and PC-emission exposed animals (G: ^ different than 1 d same exposure, $p < 0.05$). However, after 1 and 30 d exposures, the reduction in internal diameter of arteries was greater in PC-exposed than control animals (*different than same day controls, $p < 0.05$). This was accompanied by a decrease after 1 day exposure to PC-emissions and an elevation after 15 and 30 day exposures to PC-emission in the thickness of the vascular smooth muscle (green lines in E show where thickness measurements were taken; * different than same day control $p < 0.05$; ^ different than 1d same exposure, $p < 0.05$). All data are presented as the mean ± SEM. The bar = 50 µm.

TABLE 2. Average (± Sem) Internal and External Diameters of Arteries in Cardiac Tissue Measured in Hematoxylin and Eosin Stained Sections. Bold * Is Different Than Air Control ($p < 0.05$).

	Air control internal diameter (µm)	PC-emissions internal diameter (µm)	Air control external diameter (µm)	PC-emissions external diameter (µm)
1	474.55 (102.14)	**812.12 (68.57)***	1340.75 (98.63)	**979.17 (146.8)***
15	440.18 (72.39)	490.01 (35.02)	925.64 (107.72)	1107.20 (89.27)
30	568.80 (32.51)	**395.53 (60.16)***	1185.69 (68.51)	**875.91 (33.62)***

endothelium, the % area labeled for nitrotyrosine was elevated by PC-emission exposure on d 1, 15 and 30 exposure but the difference between air- and PC-exposed animals was only significant after 15 d (Figure 5g-l,o). In the VSM, the % area labeled with nitrotyrosine was significantly higher in PC- than air-exposed animals after 1 and 30-d exposures with PC-emissions (Figure 5g,h).

The photomicrographs in Figure 6a-f depict iNOS immunolabeling in cardiac arteries. Figure 6m demonstrates a reduction in area containing iNOS immunolabeling in the endothelial

TABLE 3. PC-Induced Changes in Transcript Expression in Cardiac Tissue. Numbers in Shaded Cells with * Are Significantly Different Than Same Day Controls ($p < 0.05$) and Numbers in Shaded Cells with ^ Are Different Than Day 1 Same Treatment Values ($p < 0.05$). Abbreviations: Catalase (*Cat*), Endothelial Nitric Oxide Synthase (*eNos*), Endothelin 1a (*Et1a*), Hypoxia-Induced Factor 1a (*Hif1a*), Vascular Endothelial Growth Factor (*Vegf*).

	1 day		15 days		30 days	
Transcript	Air	3D	Air	3D	Air	3D
Cat	1.18(0.27)	1.68 (0.62)	1.51 (0.64)	1.18 (0.60)	0.89 (0.23)	0.25 (0.12)*^
eNos	1.26 (0.40)	0.84 (0.14)	1.27 (0.33)	0.48 (0.07)*	1.32 (0.12)	0.80 (0.16)*
Et1a	1.12 (0.23)	1.01 (0.19)	1.36 (0.54)	0.63 (0.15)	1.12 (0.19)	2.29 (0.67)^
Hif1	1.48 (0.53)	1.31 (0.68)	1.17 (0.28)	1.00 (0.16)	0.81 (0.26)	2.88 (0.94)*^
Vegf	1.18 (0.28)	0.95 (0.13)	1.14 (0.26)	0.98 (0.15)	1.08 (0.18)	1.49 (0.41)

layer of cardiac arteries between 1- and 15-d exposures, iNOS returned to 1-d levels after 30-d exposures. iNOS in the VSM did not change in either the air- or PC-emission exposed groups at any timepoint (Figure 6n). Differences in iNOS staining in controls between days 1 and 15 may be due to the fact that these measures were made in a different group of animals (this is why there is a control at each time point). There could be different baseline levels in different groups of animals. Photomicrographs of eNOS staining are depicted in Figure 6g-l. After 15-d exposure to air, eNOS immunolabeling was lower in the endothelial layer of cardiac arteries than it was after 1 d (Figure 6o). eNOS in endothelial cells also decreased after 15- and 30-d exposures with PC as compared to after 1 d, but this difference was not significant. In addition, after 15- and 30-d exposure to PC-emissions, eNOS in the VSM was lower than it was after 1 d, but this difference was only significant after 30-d treatment (Figure 6p).

Figure 7a-l are photomicrographs of androgen receptor (AR; A-F) and vascular endothelial growth factor (VEGF; G-L) in cardiac arteries. Although there were PC-emission-induced changes in AR immunostaining in the endothelium, these alterations were not significant (Figure 7m). In the VSM (Figure 7n), there was an initial decrease in PC-emission-induced AR staining, but after 15-and 30-d treatment AR immunostaining was elevated in PC-emission exposed animals. There was also variability in AR staining in the VSM of controls, but this was primarily on day 15. Similar changes were noted in the VSM of arteries from control muscles; however, the reduction occurred later, after 15 d of exposure, with concomitant elevation after 30 days rising to equivalent levels of PC-emission exposed group. VEGF immunostaining was not markedly altered in the endothelium (Figure 7o). However, after 15-d exposures, VEGF immunostaining was reduced in the VSM of cardiac arteries of controls, but returned to 1-d levels after 30 d (Figure 7p). Differences in VEGF staining in controls between days 1 and 15 may be due to the fact that these measures were made in a different group of animals (this is why there is a control at each time point). There could be different baseline levels in different groups of animals.

In PC-emission exposed animals, VEGF immunostaining was higher in the VSM after 15-d exposure to PC-emissions than after 15-d treatment with air control, and after 30 d VEGF was higher than it was after 1-d exposure to PC-emissions (Figure 7p).

Discussion

The aims of these experiments were to determine whether (1) inhalation of PC-emissions resulted in changes in measures of peripheral and cardiovascular function and morphology that might indicate vascular and cardiovascular stress and (2) whether or not these alterations were associated with changes in steroid hormone receptors and other factors indicative of vascular and cardiovascular health. Based upon the results of these experiments, there was an effect of inhaling PC emissions on peripheral vascular function resulting in an increased responsiveness to PE after 1 and 8 d of exposure. Alterations in gene expression demonstrated that there were reductions in *Cat* and *eNos* but elevations in *Et1a* and *Hif1*. These alterations in gene expression are associated with a (1) decrease in internal diameter of cardiac arteries and thickening of the vascular smooth muscle

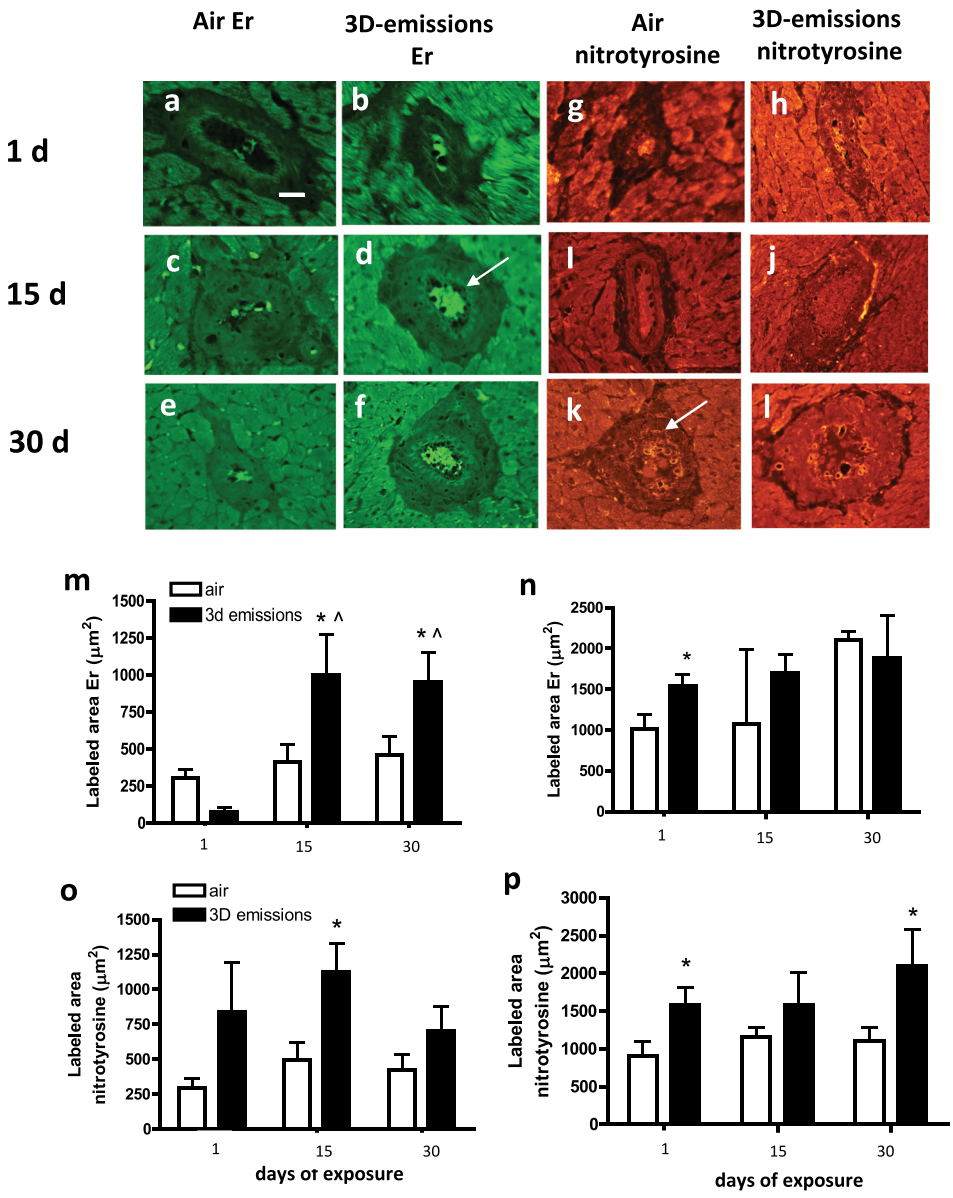

FIGURE 5. Photomicrographs of immunostaining of cardiac arteries for estrogen receptors (Er, a-f) and nitrotyrosine (g-l) in air and PC exposed animals. Following 15 and 30-d exposures to PC-emissions, there was increase in ER immunostaining in the endothelium of as compared to air control animals (D, arrow shows endothelium). However, in the vascular smooth muscle (VSM, N), exposure to PC-emissions only induced an increase in ER immunostaining after 1 d. Although it appears as if nitrotyrosine staining was enhanced in the endothelium after PC-exposure on all days, the difference was only significant after 15 d (o). The effects of PC-exposure on nitrotyrosine staining in the VSM was similar to those staining in the endothelium. However, in the VSM, nitrotyrosine staining was significantly greater in PC-exposed than air controls after 1 and 30 d. Data are presented as the average area stained (± SEM). Arrows designate the endothelium, the bar = 50 µm, and * different than air controls, $p < 0.05$ and ^ is different than 1d same treatment, $p < 0.05$.

wall in arteries of the heart, and (2) an increase in ERα staining in the coronary vascular endothelium after 15- and 30-d treatment. Changes in AR differed from what was observed with ERα in that there was an initial reduction in receptor expression in the VSM after 1 day of exposure to PC-emissions, followed by a rise in AR 15 and 30 d after treatment. There were also changes in AR staining in the VSM of controls. Because the animals in this study were still showing signs of reproductive development (all were post-pubertal, but there were endocrine changes suggesting reproductive growth; Krajnak et al. 2023), it is difficult to differentiate between developmental and exposure-related changes in steroid receptor staining, especially with AR. However, a balance between the

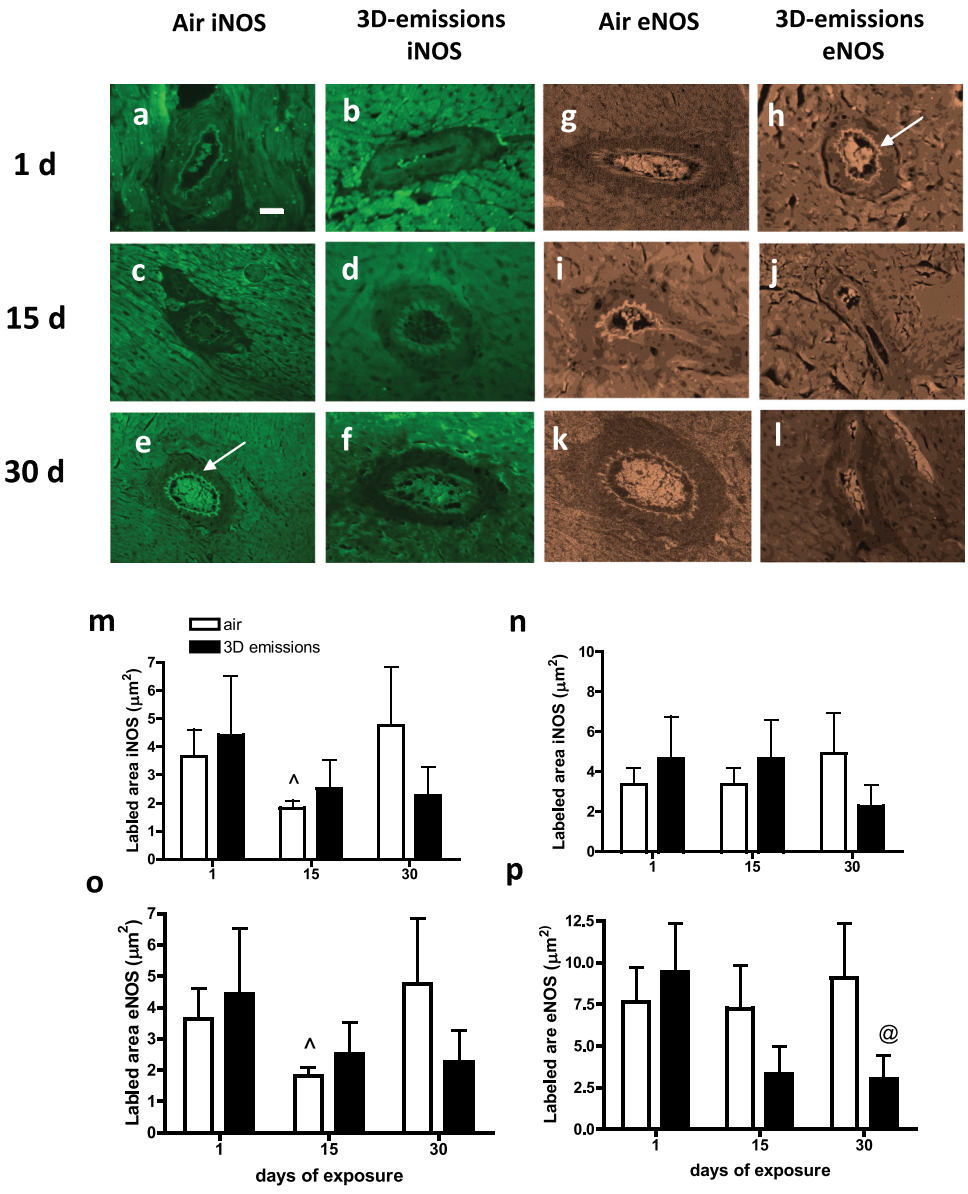

FIGURE 6. Photomicrographs of immunostaining of cardiac arteries for inducible nitric oxide synthase (iNOS, A-F) and endothelial nitric oxide synthase (eNOS; G-L) in air- and PC-exposed animals. Although there were fluctuations in iNOS staining in the endothelium (M) and VSM (N) with exposure to PC-emissions, and over time, the only significant difference was that after 15-d exposure, iNOS staining was lower in the endothelium of air exposed animals as compared to 1-d treated animals. In contrast, eNOS was reduced in both endothelium and VSM (O and P) after 15- and 30-d exposures to PC-emissions. However, in the VSM, nitrotyrosine staining was significantly greater in PC-exposed than air controls after 1- and 30-d treatment. Arrows designate the endothelium, the bar = 50 µm, and * different than air controls, $p < 0.05$. eNOS staining in the endothelium and VSM was lower in PC-exposed as compared to same day air controls, and it was lower after 15- and 30-d exposures to PC-emissions than after 1 day. Data are presented as the average area stained (± SEM). Arrow designates endothelium; bar = 50 µm; * different than same day control, $p < 0.05$; @ different than same day control, $p < 0.05$; ^ different than day 1 same treatment, $p < 0.05$).

activity of estradiol and androgens and their receptors exert effects on cardiovascular function (Huxley 2007; Lundberg et al. 1990). In addition, the increase in ERα staining in the endothelium appeared to be due to exposure to PC emissions. Additional studies examining longer exposures in older animals may help clarify how PC emissions and BPA in these emissions affect steroid-mediated alterations in cardiovascular function in the heart.

There was also a transient increase in nitrotyrosine in the VSM after 1-d exposure to PC-emissions, and in the endothelium after 15 d, suggesting that treatment with PC-emissions significantly enhanced oxidative stress. Changes in

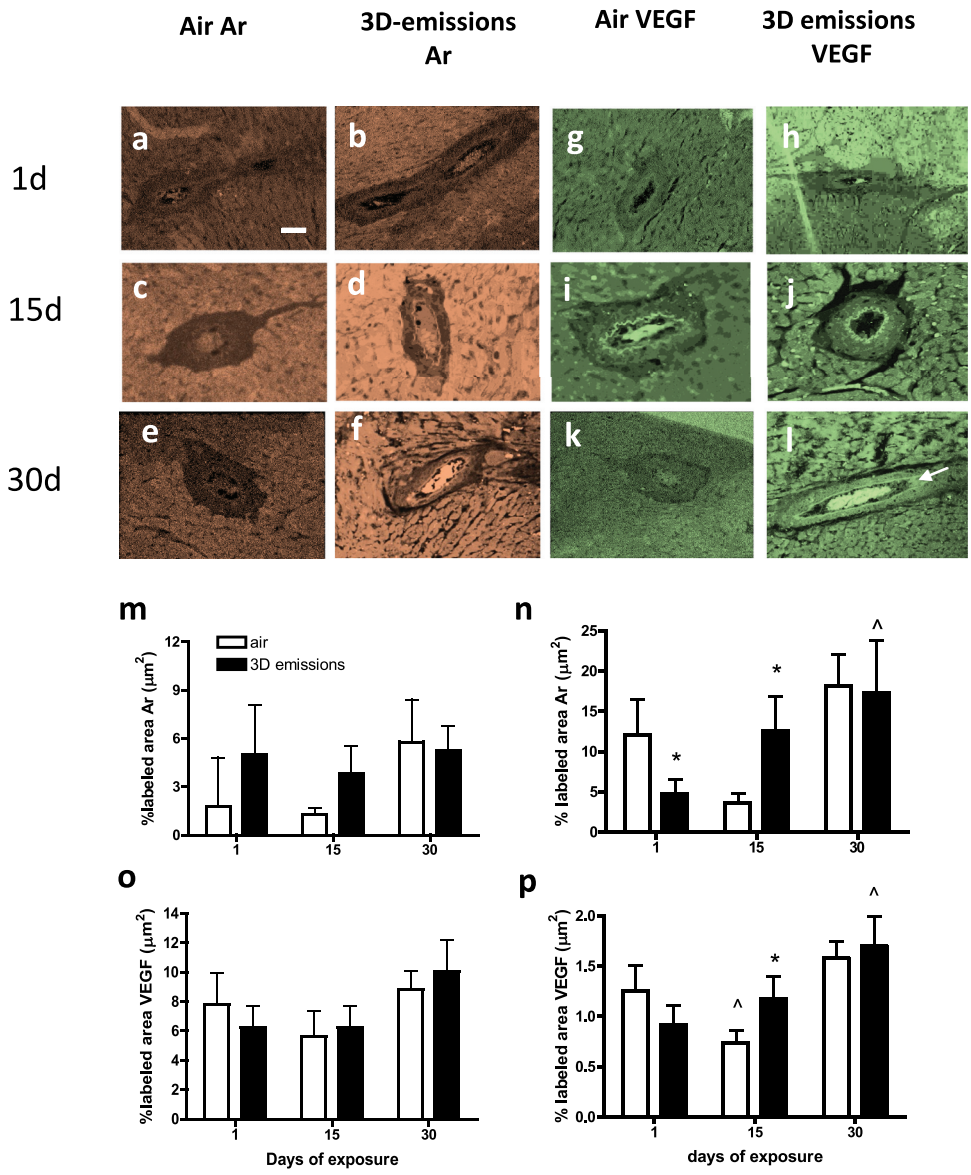

FIGURE 7. Photomicrographs of immunostaining of cardiac arteries for androgen receptors (AR, A-F) and vascular endothelial growth factor (VEGF; G-L) in air and PC exposed animals. Exposure to PC-emissions did not significantly affect AR-immunostaining in the endothelium of arteries (M). However, after 1 d treatment with PC-emission, AR was significantly reduced in the VSM. This was reversed after 15 and 30 d exposure to PC-emissions, AR immunostaining was significantly elevated in the VSM of PC-exposed animals as compared to controls (N), and Ar higher after 15 and 30 d than after 1 d. VEGF immunostaining in the endothelium did not change markedly with exposure to PC-emissions (O). VEGF in the VSM of arteries gradually rose with exposure to PC-emissions, and after 30 d, VEGF was higher than after 1 d. There was a reduction in VEGF-immunostaining in the VSM after 15 d in air controls, but after 30 d air exposure, VEGF staining returned to levels similar to those seen after 1 d air exposure (P). Data are presented as the average area stained (± SEM). Arrow designates endothelium; bar = 50 µm; * different than same day control, $p < 0.05$; ^ different than day 1 same treatment, $p < 0.05$).

measures of oxidative stress, including peroxynitrite and hydrogen peroxide might result in a reduction in oxygen that is available for nitric oxide (NO) production, or there may be an elevation in scavenging of NO to obtain oxygen for ROS production (Kotsonis et al. 1999; Phillips, Suylvester, and Frisbee 2005). Increases in ROS might also interfere with the activity of tetrahydrobiopterin, the enzyme regulating NO synthesis (Kuzkaya et al. 2003; Xia et al. 1996). Increases in ROS concentrations in the heart are known to be associated with altered cardiovascular functions and data suggest that exposure to 3D emissions, and potentially BPA found within these emissions

might contribute to a rise in markers of oxidative stress, including transcription of factors regulating ROS production, which play a role in development of cardiovascular dysfunction (Stefaniak et al. 2017; Yi et al. 2016).

Previously, Krajnak et al (2020, 2022). reported that changes in peripheral vascular function were associated with alterations in measures of cardiac function. There was an enhanced sensitivity to PE-induced vasoconstriction in the ventral tail artery in PC-exposed animals. It is possible similar changes occurred in cardiac arteries, and this resulted in vasoconstriction detected in arteries examined in histological samples. However, other vascular beds in the body possess different receptors and are differentially affected by alterations in blood pressure and consequently may be differentially affected by various factors. For example, Stefaniak et al (2017) noted that smaller resistance vessels in skeletal muscle exhibit reduced sensitivity to ACh-induced vasodilation after exposure to particulate generated by 3D printing. Future studies need to be conducted to examine the responses of different vascular beds to higher doses and/or longer exposure durations to PC-emissions.

This study did not directly measure cardiac function following exposure to PC-emissions. However, measures of various factors associated with development of cardiovascular function were analyzed. Exposure to PC-emissions resulted in a chronic vasoconstriction of cardiac arteries as evidenced by a reduction in the internal diameter and elevation in thickness of the VSM. This persistent vasoconstriction was associated with an increase in nitrotyrosine staining in both endothelium and vascular smooth muscle, indicating that there was elevated oxidative stress in cardiac arteries. Enhanced oxidative stress and elevated production of ROS most likely played a role in the sustained vasoconstriction (Gradinaru et al. 2015). Elevations in oxidative stress may result in diminished nitric oxide synthase activities. Inhibiting the activity of these enzymes can result in a sustained constriction because these enzymes are required for production of nitric oxide (NO), a major vasodilator (Bailey et al. 2005; Drożdż, Drożdż, and Wójcik 2023; Hughes et al. 2009). The generated ROS reduce NO levels because available oxygen is being used to generate more ROS. Elevations in ROS also induce increases in endothelin (*Eth1α*) in endothelial cells. All these effects might lead to sustained vasoconstriction and thickening of the VSM wall, and changes in markers of vascular stress (Drożdż, Drożdż, and Wójcik 2023; Gradinaru et al. 2015). The reduction in transcript gene expression of the anti-oxidant enzyme *catalase*, and *eNos*, and enhanced gene expression of *Hif1α* and *Eth1α* are consistent with these findings suggesting that enhanced nitrotyrosine immunostaining (indicator of elevated ROS levels) may underlie both maintained vasoconstriction and possibly, in the long term, lead to cardiovascular dysfunctions.

Decreased eNOS and iNOS immunostaining was observed in the endothelium and VSM of cardiac arteries from PC-emission-exposed animals although this decrease was not significant at each time point. The reduction in immunostaining in heart sections from PC-emission exposed animals is consistent with the observations that transcript gene expression was diminished, at least for *eNos*, and that the rise in oxidative stress not only affected gene transcription but also enzyme concentrations.

Oxidative stress may not have been the only factor inducing vasoconstriction. In a previous study, Krajnak et al (2023) reported that inhalation of PC-emissions by male rats did not markedly affect circulating estradiol concentrations, but in the current experiment, exposure to PC-emissions increased Erα-immunostaining, primarily in the vascular endothelium. Similar patterns were noted with enhanced AR immunostaining in the VSM of animals exposed to PC-emissions. Previous investigators demonstrated that estrogen might be cardio-protective in women and androgens cardio-protective in males (Huxley 2007; Lundberg et al. 1990). However, when steroid hormones or their receptors are out of the normal physiological range, these steroid hormones receptors may exert adverse pathogenic effects. Vasoconstriction of coronary arteries was found by Barbato (2009) to be affected by α2C-adrenoreceptor activity. Estradiol can act to increase α2C-adrenoreceptor numbers in VSM muscle and endothelial cells, and when an individual or animal is stressed, these receptors translocate to the cell surface, enhancing NE-mediated vasoconstriction (Bailey et al. 2005; Eid et al. 2007; Hughes et al. 2009). Increases in

steroid receptors that enhance vasoconstriction were shown to be associated with alterations in heart rate, changes in cardiac ventricular function and alterations in blood pressure (Lundberg et al. 1990). Future studies focusing on the influence of PC-emissions on steroid hormone activity and oxidative stress might provide additional information on the precise mechanisms by which these exposures may contribute to PC-emission-induced changes in cardiovascular function. Additional studies might also examine the effects of inhaling PC emissions and/or BPA during pregnancy and adolescence because the disruption of endocrine function during these periods may exert significant effects on the functioning of a number of physiological systems (Lehmler et al. 2018; National Toxicology Program 2021).

The effects of inhalation of PC-emissions were also examined on VEGF immunostaining. VEGF in the VSM increased over time in PC-emission-exposed animals. VEGF was reported to play a role in vascular remodeling, growth and survival (Meza-Alvarado et al. 2023). Although one cannot determine the precise mechanism, an elevation in VEGF might counteract the influence of a sustained vasoconstriction by increasing vascular remodeling and neovascularization. Future studies might also examine the ratio of circulating endothelin to VEGF. This ratio was found to change (more endothelin) when there is an increased risk of cardiovascular disease (Pandey et al. 2017).

Conclusions

The current study examined the effects of inhaling PC-emissions. The results were similar to those seen with the ingestion of plastic particulates (Huxley 2007; Lundberg et al. 1990), where both inhalation in the current study, and ingestion resulted in changes consistent with development of cardiovascular disease. Our study and the ingestion studies suggest that the effects may be due to exposure to plastics, and also to BPA (Cimmino et al. 2020; Mackay and Abidzaid 2018; National Toxicology Program 2021). It is also possible that the alterations in markers of cardiovascular health were affected by changes in circulating steroid and thyroid hormones (Krajnak et al. 2023). In a previous study that utilized the same group of animals, it was reported that thyroid stimulating hormone (TSH) was reduced after both 1 and 30 d of exposure to PC emissions (Krajnak et al. 2023). TSH acts by modulating thyroid hormone levels which might affect peripheral and cardiovascular function (National Toxicology Program 2021). TSH and thyroid hormone concentrations have been shown to be altered by BPA exposure (Cimmino et al. 2020; Dias et al. 2022; J.-J. Kim et al. 2020; Lehmler et al. 2018; National Toxicology Program 2021; Rochester 2013) and thereby, also potentially affect cardiovascular function in animals exposed to PC or BPA. Epidemiological evidence demonstrates that increased levels of urinary bisphenols are associated with cardiovascular disease (Dias et al. 2022; E. J. Kim et al. 2014; 2020-). Additional studies need to be conducted to determine the precise mechanism by which inhalation of PC-emissions is inducing markers of cardiovascular disease and whether these changes are due to exposure to BPA, PM, or a combination of these factors.

Disclaimer

The findings and conclusions in this paper have not been formally disseminated by the National Institute for Occupational Safety and Health or the Consumer Safety Product Commission and should not be construed to represent any agency determination or policy.

Disclosure statement

No potential conflict of interest was reported by the author(s).

Funding

This research was funded through a Cooperative Agreement the Consumer Product Safety Comission. Yong Qian was the PI on this agreement.

Data availability statement

Data will be available on the NIOSH website following publication.

References

Abraham, A., and P. Chakraborty. 2019. "A Review on Sources and Health Impacts of Bisphenol A." *Reviews on Environmental Health* 35 (2): 201–210. https://doi.org/10.1515/reveh-2019-0034.

Bailey, S. R., S. Mitra, S. Flavahan, and N. A. Flavahan. 2005. "Reactive Oxygen Species from Smooth Muscle Mitochondria Initiate Cold-Induced Constriction of Cutaneous Arteries." *American Journal of Physiology Heart & Circulatory Physiology* 289 (1): H243–H250. https://doi.org/10.1152/ajpheart.01305.2004.

Barbato, E. 2009. "Role of Adrenergic Receptors in Human Coronary Vasomotion." *Heart* 95 (7): 603–608. https://doi.org/10.1136/hrt.2008.150888.

Cimmino, I., F. Fiory, G. Perruolo, C. Miele, F. Beguinot, P. Formisano, and F. Oriente. 2020. "Potential Mechanisms of Bisphenol a (BPA) Contributing to Human Disease." *International Journal of Molecular Sciences* 21 (16): 5761. https://doi.org/10.3390/ijms21165761.

Curry, B. D., S. R. Govindaraju, J. L. W. Bain, L. L. Zhang, J.-G. Yan, H. S. Matloub, and D. A. Riley. 2005. "Evidence for Frequency-Dependent Arterial Damage in Vibrated Rat Tails." *The Anatomical Record Part A, Discoveries in Molecular, Cellular, and Evolutionary Biology* 284A (2): 511–521. https://doi.org/10.1002/ar.a.20186.

Dias, P., V. Tvrdý, W. Jirkovský, M. Sollner Dolenc, L. Peterlin Mašič, and P. Mladěnka. 2022. "The Effects of Bisphenols on the Cardiovascular System." *Critical Reviews in Toxicology* 52 (1): 66–87. https://doi.org/10.1080/10408444.2022.2046690.

Drożdż, D., M. Drożdż, and M. Wójcik. 2023. "Endothelial Dysfunction As a Factor Leading to Arterial Hypertensions." *Pediatric Nephrology* 38 (9): 2973–2985. https://doi.org/10.1007/s00467-022-05802-z.

Eid, A. H., K. Maiti, S. Mitra, M. A. Chotani, S. Flavahan, S. R. Bailey, C. S. Thompson-Torgerson, and N. A. Flavahan. 2007. "Estrogen Increases Smooth Muscle Expression of α 2C -Adrenoceptors and Cold-Induced Constriction of Cutaneous Arteries." *American Journal of Physiology Heart & Circulatory Physiology* 293 (3): H1955–H1961. https://doi.org/10.1152/ajpheart.00306.2007.

Farcas, M. T., W. McKinney, W. K. Mandler, A. K. Knepp, L. Batelli, S. A. Friend, A. B. Stefaniak, et al. 2024. "2024Pulmonary Evaluation of Whole-Body Exposure of Polycarbonate (PC) Filament 3D Printer Emissions in Rats." *Journal of Toxicology and Environmental Health Part A* 87 (8): 325–341. https://doi.org/10.1080/15287394.2024.2311170.

Farcas, M. T., W. McKinney, C. Qic, W. K. Mandler, S. A. Friend, A. Stefaniak, M. Jackson, et al. 2020. "Pulmonary and Systemic Toxicity in Rats Following Inhalation Exposure of 3-D Printer Emissions from Acrylonitrile Butadiene Styrene (ABS) Filament." *Inhalation Toxicology* 32 (11–12): 403–418. https://doi.org/10.1080/08958378.2020.1834034.

Farcas, M. T., A. B. Stefaniak, A. K. Knepp, W. K. Mandler, M. Kashon, S. R. Jackson, T. A. Stueckle, et al. 2019. "Acrylonitrile Butadiene Styrene (ABS) and Polycarbonate (PC) Filaments Three-Dimensional (3-D) Printer Emissions-Induced Cell Toxicity." *Toxicology Letters* 317:1–12. https://doi.org/10.1016/j.toxlet.2019.09.013.

Gradinaru, D., C. Borsa, C. Ionescu, and G. I. Prada. 2015. "Oxidized LDL and NO Synthesis—Biomarkers of Endothelial Dysfunction and Ageing." *Mechanisms of Ageing and Development* 151:101–113. https://doi.org/10.1016/j.mad.2015.03.003.

Hubbs, A. F., R. R. Mercer, S. A. Benkovic, J. Harkema, K. Sriram, D. Schwegler-Berry, M. P. Goravanahally, T. R. Nurkiewicz, V. Castranova, and L. M. Sargent. 2011. "Nanotoxicology—A Pathologist's Perspective." *Toxicologic Pathology* 39 (2): 301–324. https://doi.org/10.1177/0192623310390705.

Hughes, J. M., O. Wirth, K. Krajnak, R. Miller, S. Flavahan, D. E. Berkowitz, D. Welcome, and N. A. Flavahan. 2009. "Increased Oxidant Activity Mediates Vascular Dysfunction in Vibration Injury." *Journal of Pharmacology and Experimental Therapeutics* 328 (1): 223–230. https://doi.org/10.1124/jpet.108.144618.

Huxley, V. H. 2007. "Sex and Cardiovascular System: The Intriguing Tale of How Women and Men Regulate Cardiovascular Function Differently." *Advances in Physiology Education* 31 (1): 17–22. https://doi.org/10.1152/advan.00099.2006.

Johnson, D. 2013. "Nanoparticles Emitted from 3D Printers Could Pose a Risk: Emission Rates Are on Par with Other Household Devices, but the Particles May Be More Toxic." *IEEE Specturm*. https://spectrum.ieee.org/nanoparticles-emitted-from-3d-printers-could-pose-a-risk.

Khraishah, H., B. Alahmad, R. L. Ostergard, A. AlAshqar, M. Albaghdadi, N. Vellanki, M. M. Chowdhury, et al. 2022. "Climate Change and Cardiovascular Disease: Implications for Global Health." *Nature Reviews Cardiology* 19 (12): 798–812. https://doi.org/10.1038/s41569-022-00720-x.

Kim, J.-J., S. Kumar, V. Kumar, Y.-M. Lee, Y.-S. Kim, and V. Kumar. 2020. "Bisphenols As a Legacy Pollutant, and Their Effects on Organ Vlulnerability." *International Journal of Environmental Research and Public Health* 17 (1): 112. https://doi.org/10.3390/ijerph17010112.

Kim, E. J., D. Lee, B. C. Chung, H. Pyo, and J. Lee. 2014. "Association Between Urinary Levels of Bisphenol-A and Estrogen Metabolism in Korean Adults." *Science of the Total Environment* 470-471:1401–1407. https://doi.org/10.1016/j.scitotenv.2013.07.040.

Kotsonis, P., A. Frey, L. G. Fröhlich, H. Hofmann, A. Reif, D. A. Wink, M. Feelisch, and H. H. Schmidt. 1999. "Autoinhibition of Neuronal Nitric Oxide Synthase: Distinct Effects of Reactive Nitrogen and Oxygen Species on Enzyme Activity." *The Biochemical Journal* 340 (3): 745–752. https://doi.org/10.1042/bj3400745.

Krajnak, K., R. G. Dong, S. Flavahan, D. Welcome, and N. A. Flavahan. 2006. "Acute Vibration Increases α 2C -

Adrenergic Smooth Muscle Constriction and Alters Thermosensitivity of Cutaneous Arteries." *Journal of Applied Physiology* 100 (4): 1230–1237. https://doi.org/10.1152/japplphysiol.00761.2005.

Krajnak, K., M. Farcas, J. Richardson, M. A. Hammer, S. Waugh, W. McKinney, M. Jackson, D. Matheson, T. Thomas, and Y. Qian. 2023. "Inhalation of Polycarbonate Emissions Generated During 3D Printing Processes Affects Neuroendocrine Function in Male Rats." *Journal of Toxicology and Environmental Health Part A* 86 (16): 575–596. https://doi.org/10.1080/15287394.2023.2226198.

Krajnak, K., H. Kan, K. A. Russ, W. McKinney, S. Waugh, W. Zheng, M. L. Kashon, C. Johnson, J. Cumpston, and J. S. Fedan. 2020. "Biological Effects of Inhaled Hydraulic Fracturing Sand Dust. VI. Cardiovascular Effects." *Toxicology & Applied Pharmacology* 406:115242. https://doi.org/10.1016/j.taap.2020.115242.

Krajnak, K., G. R. Miller, S. Waugh, C. Johnson, and M. L. Kashon. 2010. "Characterization of Frequency-Dependent Responses of the Sensorineural System to Repetitive Vibration." *Journal of Occupational & Environmental Medicine / American College of Occupational & Environmental Medicine* 54 (8): 1010–1016. https://doi.org/10.1097/JOM.0b013e318255ba74.

Krajnak, K., K. A. Russ, W. McKinney, S. Waugh, W. Zheng, H. Kan, M. L. Kashon, J. Cumpston, and J. S. Fedan. 2022. "Biological effects of crude oil vapor. IV. Cardiovascular effects." *Toxicology & Applied Pharmacology* 447:116071. https://doi.org/10.1016/j.taap.2022.116071.

Krajnak, K., K. Sriram, C. Johnson, J. R. Roberts, R. R. Mercer, G. R. Miller, O. Wirth, and J. M. Antonini. 2017. "Effects of Pulmonary Exposures to Chemically-Distinct Welding Fumes on Neuroendocrine Markers of Toxicity." *Journal of Toxicology and Environmental Health Part A* 80 (5): 301–314. https://doi.org/10.1080/15287394.2017.1318324.

Krajnak, K., S. Waugh, C. Johnson, G. R. Miller, X. Xu, C. Warren, and R. G. Dong. 2013. "The Effects of Impact Vibration in Peripheral Blood Vessles and Nerves." *Industrial Health* 51 (6): 572–580. https://doi.org/10.2486/indhealth.2012-0193.

Krajnak, K., S. Waugh, R. Miller, B. Baker, K. Geronilla, S. E. Alway, and R. G. Cutlip. 2006. "Acute Vibration Reduces Aβ Nerve Fiber Sensitivity and Alters Gene Expression in the Ventral Tail Nerves of Rats." *Muscle & Nerve* 36 (2): 197–205. https://doi.org/10.1002/mus.20804.

Kuzkaya, N., N. Weissmann, D. G. Harrison, and S. Dikalov. 2003. "Interactions of Peroxynitrite, Tetrahydrobiopterin, Ascorbic Acid, and Thiols: Implications for Uncoupling Endothelial Nitric-Oxide Synthase." *Journal of Biological Chemistry* 278 (25): 22546–22554. https://doi.org/10.1074/jbc.M302227200.

Lehmler, H., J. Liu, B. Gadogbe, and W. Bao. 2018. "Exposure to Bisphenol A, Bisphenol F, and Bisphenol S in U.S. Adults and Children: The National Health and Nutrition Examination Survey 2013–2014." *American Chemical Society Omega* 3 (6): 6523–6532. https://doi.org/10.1021/acsomega.8b00824.

Lundberg, U., L. Wallin, G. Lindstedt, and M. Frankenhaueser. 1990. "Steroid Sex Hormones and Cardiovascular Function in Health Males and Females: A Correlational Study." *Pharmacology, Biochemistry, and Behavior* 37 (2): 325–327. https://doi.org/10.1016/0091-3057(90)90342-F.

Mackay, H., and A. Abidzaid. 2018. "A Plurality of Molecular Targets: The Receptor Ecosytem for Bisphenol-A (BPA)." *Hormones and Behavior* 101:59–67. https://doi.org/10.1016/j.yhbeh.2017.11.001.

Ma, Y., H. Liu, J. Wu, L. Yuan, Y. Wang, X. du, R. Want, et al. 2019. "The Adverse Health Effects of Bisphenol a and Related Toxicity Mechanisms." *Environmental Research* 176:108575. https://doi.org/10.1016/j.envres.2019.108575.

Meza-Alvarado, J. C., R. A. Page, B. Mallard, C. Bromhead, and B. R. Palmer. 2023. "VEGF- a Related SNPs: A Cardiovascular Context." *Frontiers in Cardiovascular Medicine* 10. https://doi.org/10.3389/fcvm.2023.1190513.

NTP (National Toxicology Program). 2021. "NTP Research Report on the Consortium Linking Academic and Regulatory Insights on Bisphenol a Toxicity (CLARITY-BPA): A Compendium of Published Findings." Research Triangle Park, North Carolina.

Pandey, A. K., E. K. Singhi, J. P. Arroyo, T. A. Ikizler, E. R. Gould, J. Brown, J. A. Beckman, D. G. Harris, and J. Moslehi. 2017. "Mechanisms of VEGF (Vascular Endothelial Growth Factor) Inhibitor–Associated Hypertension and Vascular Disease." *Hypertension* 71 (2): e1–e8. https://doi.org/10.1161/HYPERTENSIONAHA.117.10271.

Phillips, S. A., F. A. Suylvester, and J. C. Frisbee. 2005. "Oxidant Stress and Constrictor Reactivity Impair Cerebral Artery Dilation in Obese Zucker Rats." *American Journal of Physiology Regulatory, Integrative and Comparative Physiology* 288 (2): R522–30. https://doi.org/10.1152/ajpregu.00655.2004.

Roberts, J. R., S. E. Anderson, H. Kan, K. Krajnak, J. A. Thompson, A. Kenyon, W. T. Goldsmith, et al. 2014. "Evaluation of Pulmonary and Systemic Toxicity of Oil Dispersant (COREXIT EC9500A((R))) Following Acute Repeated Inhalation Exposure." *Environmental Health Insights* 8 (Suppl 1): 63–74. https://doi.org/10.4137/EHI.S15262.

Rochester, J. A. 2013. "Bisphenol a and Human Health: A Review of the Literature." *Reproductive Toxicology (Elmsford, NY)* 42:132–155. https://doi.org/10.1016/j.reprotox.2013.08.008.

Sanchez, P., B. Castro, S. Martinez-Rodriguez, R. Rios-Pelegrina, R. G. del Moral, J. M. Torres, and E. Ortega. 2022. "Impact of Chronic Exposure of Rats to Bisphenol a from Perinatal Period to Adulthood on Intraprostatic Levels of 5α-Reductase Isozymes, Aromatase, and Genes Implicated in Prostate Cancer Development." *Environmental Research* 212 (Part A): 113142. https://doi.org/10.1016/j.envres.2022.113142.

Secondo, L. E., H. I. Adawi, J. Cuddehe, J. K. Hopson, A. Schumacher, L. Mendoza, C. Cartin, and N. A. Lewinskin. 2020. "Comparative Analysis of Ventilation Efficiency on Ultrafine Particle Removal in University Makerspaces." *Atmospheric Environment* 224:117321. https://doi.org/10.1016/j.atmosenv.2020.117321.

Shivika, S., and C. Subhankar. 2017. "Microplastic Pollution, a Threat to Marine Ecosystem and Human Health: A Short Review." *Environmental Science and Pollution Research* 24 (27): 21530–21547. https://doi.org/10.1007/s11356-017-9910-8.

Stefaniak, A. B., S. du Preez, and J. L. du Plessis. 2021. "Additive Manufacturing for Occupational Hygiene: A Comprehensive Review of Processes, Emissions and Exposures." *Journal of Toxicology and Environmental Health, Part B* 24 (5): 173–222. https://doi.org/10.1080/10937404.2021.1936319.

Stefaniak, A. B., R. F. LeBouf, M. G. Duling, J. Yi, A. B. Abukabda, C. R. McBride, and T. R. Nurkiewicz. 2017. "Inhalation Exposure to Three-Dimensional Printer Emissions Stimulates Acute Hypertension and Microvascular Dysfunction." *Toxicology and Applied Pharmacology* 335:1–5. https://doi.org/10.1016/j.taap.2017.09.016.

Stephens, B., P. Azimi, Z. E. Orch, and T. Ramos. 2013. "Ultrafine paticle emissions from destop 3D printers." *Atmospheric Environment* 79:334–339. https://doi.org/10.1016/j.atmosenv.2013.06.050.

Tarskikh, M. M., L. G. Klimatskaya, and S. I. Kolesnikov. 2013. "Pathogenesis of Neurotoxicity of Acrylates Acrylonitrile and Acrylamide: From Cell to Organism." *Bulletin of Experimental Biology and Medicine* 155 (4): 451–453. https://doi.org/10.1007/s10517-013-2175-4.

Väisänen, A., L. Alonen, S. Ylönen, and M. Hyttinen. 2022. "Organic Compound and Particle Emissions of Additive Manufacturing with Photopolymer Resins and Chemical Outgassing of Manufactured Resin Products." *Journal of Toxicology and Environmental Health Part A* 85 (5): 198–216. https://doi.org/10.1080/15287394.2021.1998814.

Xia, Y., V. L. Dawson, T. M. Dawson, S. H. Snyder, and J. L. Zweier. 1996. "Nitric Oxide Synthase Generates Superoxide and Nitric Oxide in Arginine-Depleted Cells Leading to Peroxynitrite-Mediated Cellular Injury." *Proceedings of the National Academy of Sciences* 93 (13): 6770–6774. https://doi.org/10.1073/pnas.93.13.6770.

Yi, J., R. F. LeBouf, M. G. Duling, T. Nurkiewicz, B. T. Chen, D. Schwegler-Berry, M. A. Virji, and A. B. Stefaniak. 2016. "Emission of Particulate Matter from a Desktop Three-Dimensional (3D) Printer." *Journal of Toxicology and Environmental Health Part A* 79 (11): 453–465. https://doi.org/10.1080/15287394.2016.1166467.